

# Mullite–Aluminosilicate Glassy Matrix Substrates Obtained by Reactive Coating

J. Requena,<sup>a</sup> J. F. Bartolomé,<sup>a</sup> J. S. Moya,<sup>a</sup> S. de Aza,<sup>a</sup> F. Guitian<sup>b</sup> & G. Thomas<sup>c</sup>

<sup>a</sup>Instituto de Cerámica y Vidrio (CSIC), Arganda del Rey, Madrid, Spain

<sup>b</sup>Instituto de Cerámica, Universidad de Santiago, Spain

<sup>c</sup>Department of Materials Science and Mineral Engineering, University of California, Berkeley, CA 94720, USA

(Accepted 22 July 1995)

## Abstract

*Layered kaolinite–alumina composites have been obtained by a sequential slip casting technique. The interfacial reaction as well as the microstructure of different layers have been studied in laminates fired at 1650°C. The results are discussed on the basis of the  $\text{SiO}_2\text{--Al}_2\text{O}_3\text{--K}_2\text{O}$  equilibrium diagram. Taking into account these results, a new low-cost ceramic substrate for electronic applications — reinforced by mullite whiskers and with controlled closed porosity, low permittivity value ( $\epsilon \approx 4$  at 1 MHz) and thermal expansion coefficient close to that of silicon ( $3.8 \times 10^{-6} \text{ }^\circ\text{C}^{-1}$ ) — has been developed starting from conventional kaolinite powder.*

## Introduction

Recently, Liu *et al.*<sup>1,2</sup> have studied mullite formation in the alumina–kaolinite system. By X-ray diffraction (XRD) and transmission electron microscopy (TEM) analysis, they have clearly shown the formation of monosized primary mullite in plate-like kaolinite at 1300°C. At higher temperatures bimodal mullite crystals were detected, indicating formation of secondary mullite by nucleation and primary mullite growth. This secondary mullite is formed mainly by a solution–precipitation mechanism. Both types of mullite have a different composition and different morphologies. Primary mullite is needle-like with [001] being the crystallographic growth direction.<sup>3</sup> The secondary mullite has a higher content of alumina and no preferential growth direction.

In the present work kaolinite has been spatially separated from alumina by means of a layered structure obtained by sequential slip casting. In this configuration, the interfacial reaction, microstructure development into the layers and morphological

aspects of the fired composites have been studied. On the basis of the results obtained, a new substrate with low permittivity value is proposed for electronic applications.

## Experimental

The following starting materials have been used: (1) high-purity kaolinite (Caobar S.A., Spain) with an average particle size of 3  $\mu\text{m}$  and a specific surface area of 9.2  $\text{m}^2 \text{g}^{-1}$ , with mica and quartz as minor constituents; and (2) commercial submicronic alumina (Alcoa CT 3000 SG) with an average particle size of 0.5  $\mu\text{m}$  and a specific surface area of 8.0  $\text{m}^2 \text{g}^{-1}$ . The results of wet chemical analysis (wt%) of both materials are (1) Caobar kaolinite:  $\text{SiO}_2$  (48.4),  $\text{Al}_2\text{O}_3$  (37.0),  $\text{Fe}_2\text{O}_3$  (0.25),  $\text{TiO}_2$  (0.002),  $\text{Na}_2\text{O}$  (0.13),  $\text{K}_2\text{O}$  (0.46),  $\text{CaO}$  (0.31),  $\text{MgO}$  (0.05) and (2)  $\alpha$ -alumina:  $\text{Al}_2\text{O}_3$  (99.2),  $\text{Na}_2\text{O}$  (0.12),  $\text{SiO}_2$  (0.08),  $\text{MgO}$  (0.1) and  $\text{Fe}_2\text{O}_3$  (0.03). Aqueous suspensions were prepared of alumina and kaolinite, using an alkali-free organic polyelectrolyte in the case of alumina and sodium silicate and sodium carbonate in the case of kaolinite. Both suspensions were dispersed in alumina ball mills for 4 h. The suspensions showed Newtonian flow behaviour and low viscosity values (i.e. 11 and 15  $\text{mPa s}^{-1}$  for  $\text{Al}_2\text{O}_3$  and kaolinite, respectively).

Multilayer alumina–kaolinite composites were obtained by alternately casting alumina and kaolinite suspensions in plaster of Paris moulds according to the flow chart shown in Fig. 1.

Microstructural analysis was performed on polished cross-sections with and without chemical etching (10% HF solution) using optical microscopy (Zeiss Axiophot, Germany) with an image analyser, and scanning electron microscopy (SEM) with EDS and WDS (Jeol JMS-6400, Japan).

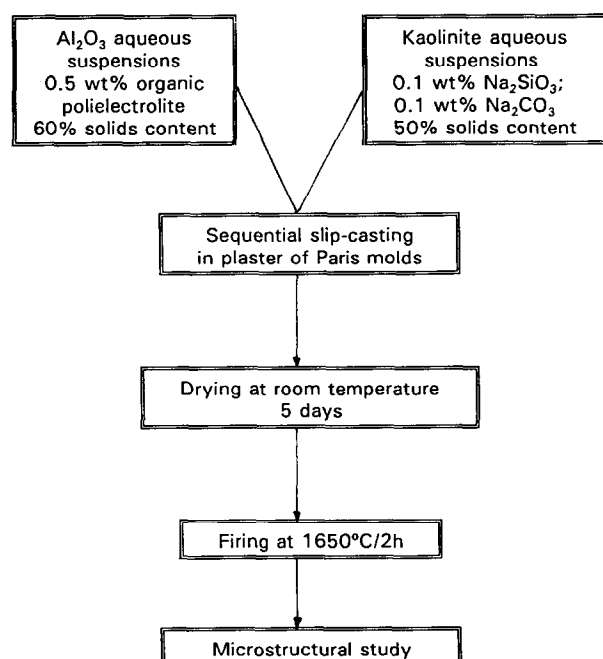


Fig. 1. Processing flow chart for layered composites.

## Results and Discussion

### Layered composites

The cross-section of a layered composite after firing is shown in Fig. 2. As observed, the morphology of the laminate is built up of dense alumina layers and porous aluminosilicate (original kaolinite) layers. Cracks due to the thermal expansion mismatch are visible.

SEM micrographs of polished and chemically etched surfaces are shown in Fig. 3. It is seen that the interface is formed by a  $\sim 5 \mu\text{m}$  layer of secondary mullite which penetrates into the alumina

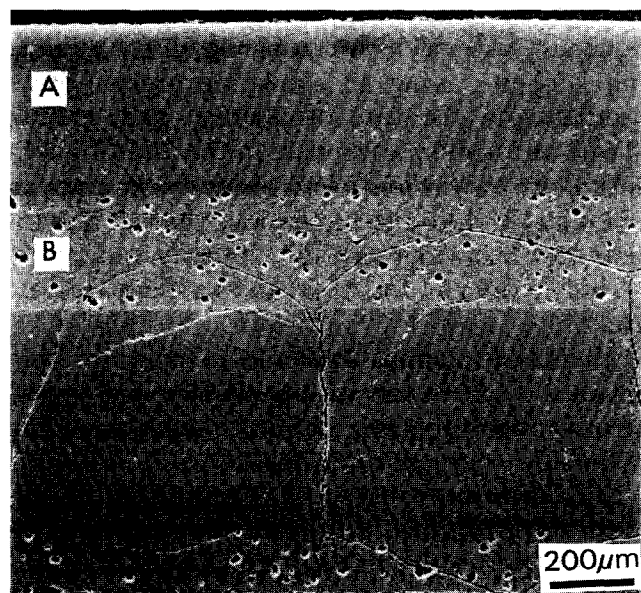


Fig. 2. SEM micrographs of the alumina-kaolinite multilayer composite fired at 1650°C: (A) alumina layer; (B) original kaolinite layer.

Table 1. Quantitative microprobe (WDX) analysis (wt%)

	$\text{Al}_2\text{O}_3$	$\text{SiO}_2$	$\text{K}_2\text{O}$
Primary mullite	$72.0 \pm 0.5$	$26.6 \pm 0.3$	—
Secondary mullite	$73.5 \pm 0.3$	$27.8 \pm 0.3$	—
Glassy matrix*	$26.4 \pm 0.7$	$73.88 \pm 0.56$	$1.47 \pm 0.05$

\*CaO and  $\text{Fe}_2\text{O}_3$  impurities have not been considered.

layer, entrapping alumina grains. The original kaolinite layer transforms into a silica-rich glassy matrix containing aluminium, potassium, calcium and iron, as can be seen in the corresponding EDS pattern, and prismatic primary mullite crystals. EDS spectra corresponding to primary and secondary mullite are also shown.

This particular microstructure can be explained by means of the  $\text{SiO}_2$ - $\text{Al}_2\text{O}_3$ - $\text{K}_2\text{O}$  equilibrium phase diagram.<sup>4</sup> In Fig. 4 the silica-alumina-rich portion of this diagram is plotted. The theoretical composition of metakaolinite as well as the composition of the calcined Caobar kaolinite have also been plotted. In this plot only the  $\text{K}_2\text{O}$  impurity has been taken into account. According to this equilibrium diagram, on heating, Caobar kaolinite will develop a liquid phase at the eutectic temperature ( $985^\circ\text{C}$ ) which corresponds to the invariant point of the subsystem silica-mullite-potash feldspar. As the temperature increases, the composition of the glassy phase will move along the cristobalite-mullite boundary until reaching a temperature close to  $1470^\circ\text{C}$ . Then the cristobalite disappears and the liquid phase moves away from the binary boundary following the tie-line which joins the Caobar kaolinite composition with the silica-rich mullite composition, until reaching the isothermal line corresponding to  $1650^\circ\text{C}$ , the final firing temperature. This liquid is in equilibrium with primary mullite. In a subsequent step this liquid will react with the alumina layer, giving alumina saturated with secondary mullite.

Quantitative microprobe analysis (WDS) of the primary mullite, secondary mullite and glassy matrix corresponding to the layered composites fired at  $1650^\circ\text{C}$  is reported in Table 1. As can be observed, these data are in good agreement with the previous synopsis.

### Layered substrates for electronics

One basic requirement for electronic ceramics that support high frequency circuitry,<sup>5</sup> is to have a low permittivity value ( $\epsilon$ ), to provide short signal transmission delay time ( $t_d$ ):

$$t_d = \frac{\sqrt{\epsilon s}}{c}$$

where  $s$  = signal pass length and  $c$  = velocity of light.

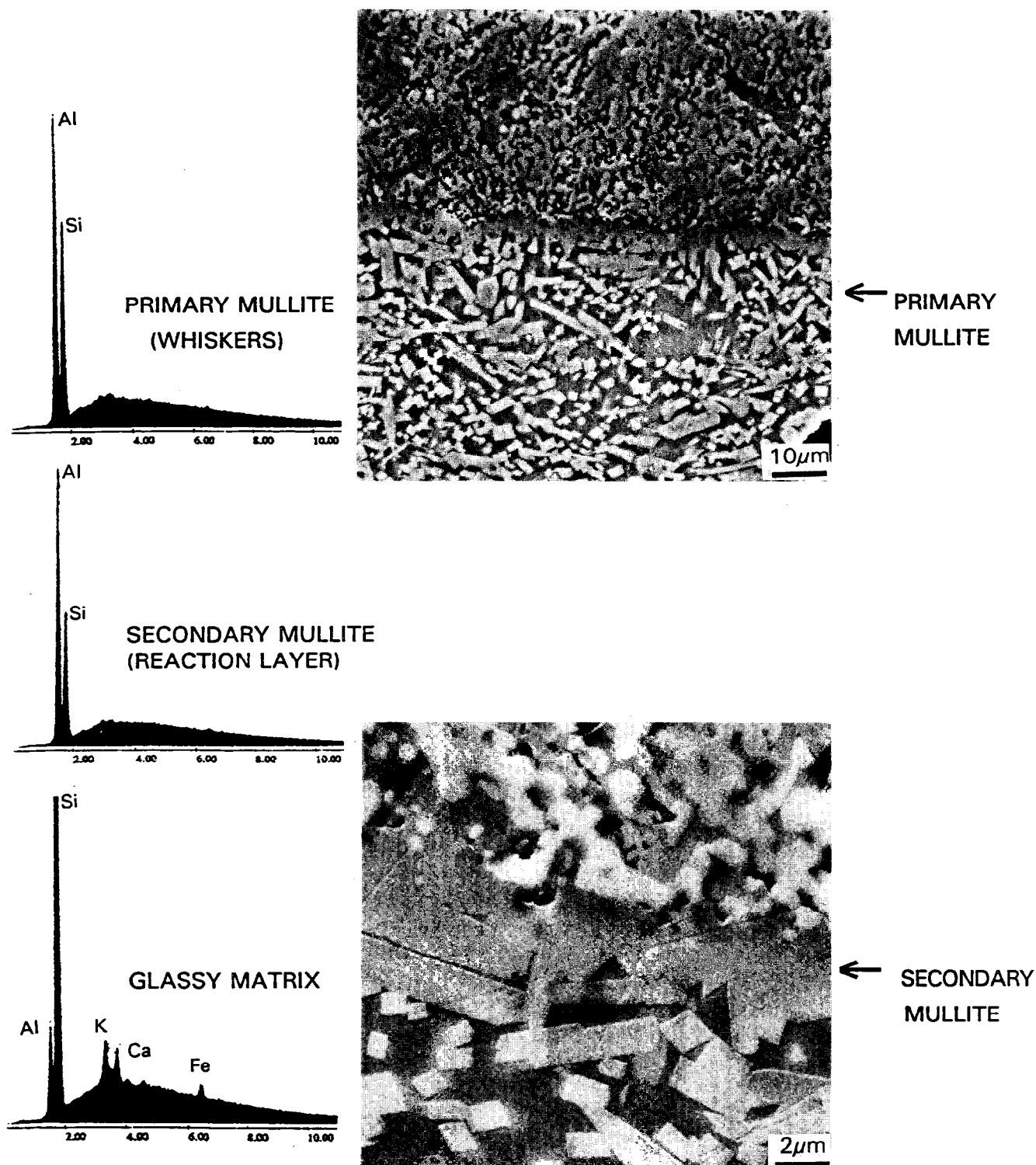


Fig. 3. SEM micrograph of polished and HF-etched cross-section of the alumina–kaolinite layered composite. The EDS spectra corresponding to primary mullite, secondary mullite and glassy matrix are also shown.

The major problems for large-scale production of mullite silica glass substrate are:<sup>6,7</sup>

- (i) high cost of starting materials;
- (ii) porosity control;
- (iii) formation of cristobalite;
- (iv) low mechanical properties.

Taking into account the results obtained in the layered composites as previously reported, it should be possible to design a silicoaluminate

glassy matrix reinforced with mullite whiskers and with controlled porosity starting from low-cost kaolinite raw materials.

The idea consists of coating a prefired kaolinite block with a sufficiently thin layer of alumina in order to develop, during final firing (at 1650°C), an electrical insulator layer of secondary mullite, avoiding the cracks formed because of the thermal expansion mismatch between alumina and silicoaluminate layers (Fig. 2).

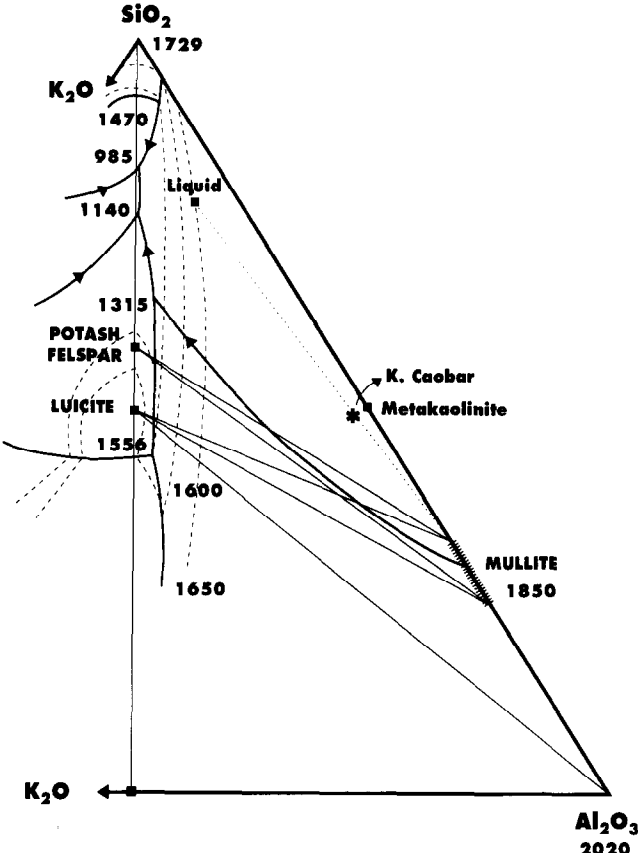


Fig. 4. The SiO<sub>2</sub>-Al<sub>2</sub>O<sub>3</sub>-K<sub>2</sub>O equilibrium diagram.

According to the equilibrium diagram plotted in Fig. 4 as well as the time-temperature-transformation curves reported by Liu *et al.*<sup>2</sup> for Caobar kaolinite (Fig. 5), if firing is made at  $T > 1470^{\circ}\text{C}$  no cristobalite is present. In this case only mullite and glassy phases are formed, as has been observed in the present case. In this sense, a processing-flow chart, as shown schematically in Fig. 6, has been followed.

Figure 7 shows an optical micrograph of the cross-section of the fired substrate. As observed, closed pores  $< 40\text{ }\mu\text{m}$  are present. The total porosity has been determined by image analysis on micrographs and found to be  $8 \pm 1\text{ vol}\%$ .

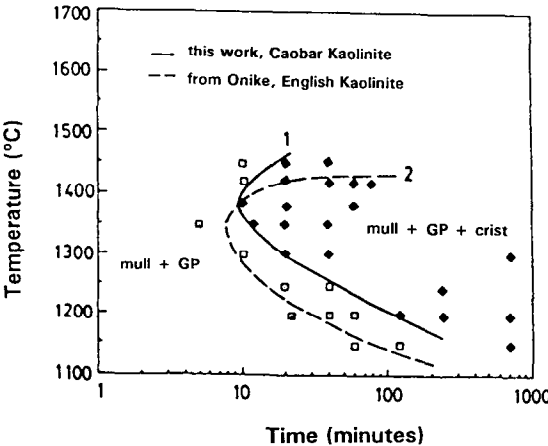


Fig. 5. Time-temperature-transformation curves of cristobalite nucleation for Caobar Kaolinite and English Kaolinite.

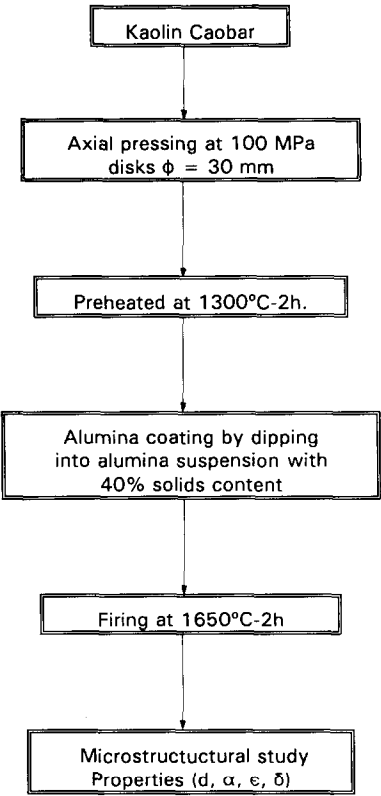


Fig. 6. Substrates processing flow chart.

The micrograph of an HF etched polished cross-section shows the presence of  $5\text{ }\mu\text{m}$  thick coating of a secondary mullite layer and a bulk formed by continuous glassy matrix reinforced by primary mullite whiskers. These are of length  $20 \pm 5\text{ }\mu\text{m}$  and width  $2 \pm 0.5\text{ }\mu\text{m}$ , having an aspect ratio of  $10 \pm 2$  (Fig. 8). The content of the primary mullite needle-like single crystals has been determined by quantitative XRD analysis and found to be 60 wt%. These data are in agreement with that calculated from Fig. 4 at  $1650^{\circ}\text{C}$  ( $60 \pm 5\%$ ).

The specific gravity of the fired substrate has

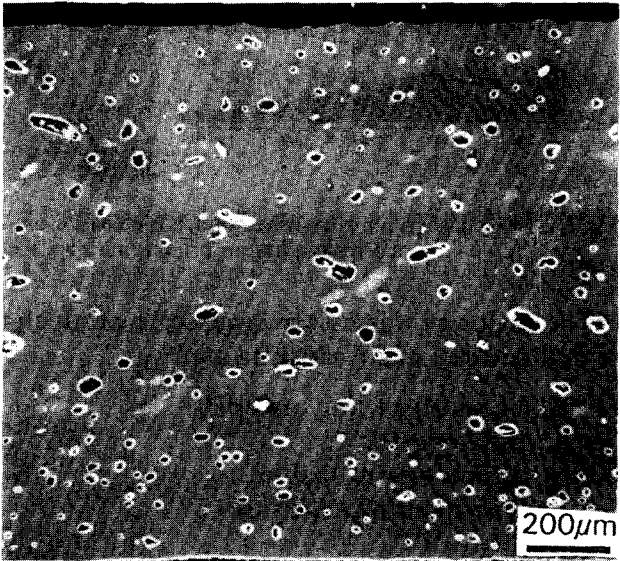
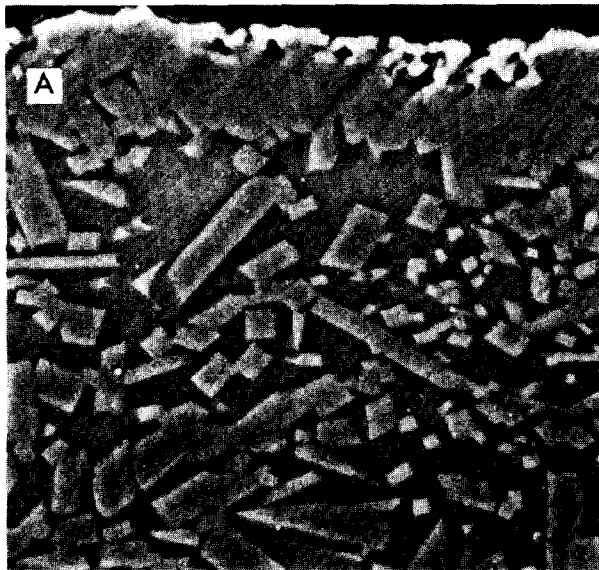
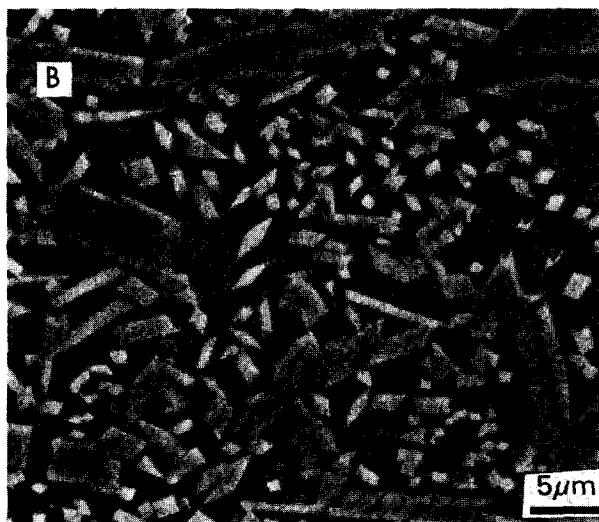


Fig. 7. Optical micrograph of the cross-section of a substrate, showing closed porosity.



SECONDARY MULLITE  
LAYER



PRIMARY MULLITE WHISKERS  
REINFORCE GLASSY MATRIX

Fig. 8. SEM micrographs of the cross-section of a substrate fired at 1650°C: (A) secondary mullite top layer; (B) glassy matrix reinforced with primary mullite whiskers.

been determined using Archimedes' method in Hg and has been found to be  $2.75 \pm 0.06 \text{ g cm}^{-3}$ .

The thermal expansion of the substrate has been determined by dilatometry using a sample of 1 cm length, giving  $\alpha_{20-500} = 3.8 \times 10^{-6} \text{ }^{\circ}\text{C}^{-1}$ . As can be observed in Fig. 9, the thermal expansion of the substrate matches that of silicon in the temperature interval ranging from 20 to 600°C.

The dielectric constant and dielectric loss were determined on discs 25 mm in diameter and 2 mm height with parallel flat surfaces coated by Ag (70 wt%) + Pd (30 wt%), the discs being heated at 200°C for 30 min prior to measurements. A Hewlett-Packard 4192 ALF impedance analyser at 1 kHz to 10 MHz at 0.1–0.2 mV was used. The results obtained were:  $\epsilon = 4$  at 1 MHz;  $\delta = 0.01$  at 1 MHz.

Tummala<sup>8</sup> has pointed out that for high performance ceramic packaging, the two main requirements are: (i) less interconnect delay and (ii) larger chip. To meet the first requirement ceramic

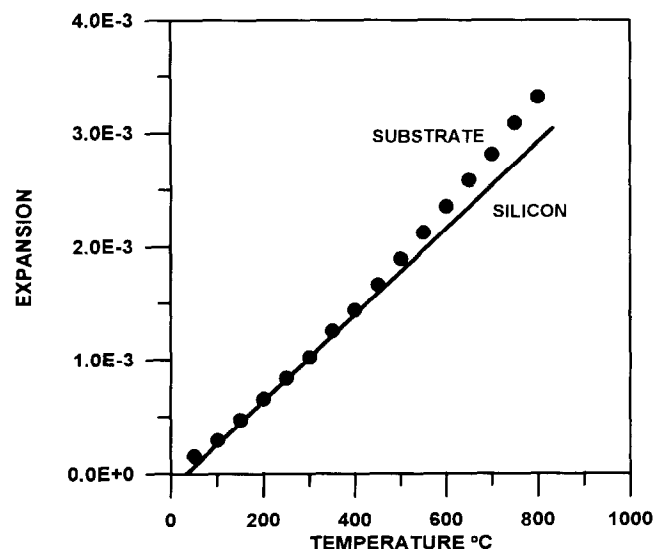


Fig. 9. Thermal expansion curve of the substrate. That of silicon is also shown for comparison purposes.

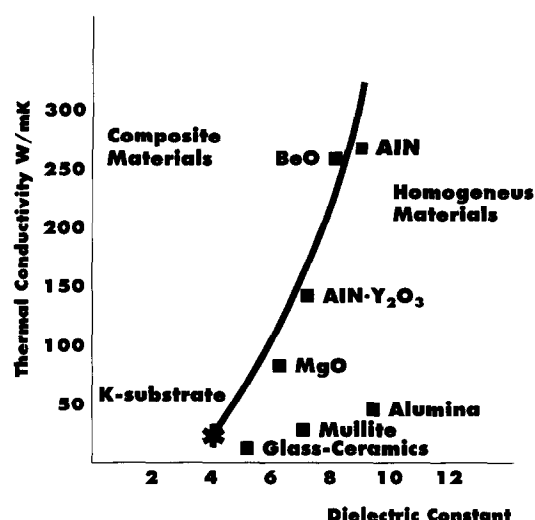


Fig. 10. Thermal conductivity versus dielectric constant for several materials used in electronic packaging. The value corresponding to the kaolinite-based substrate is also plotted (\*).

substrates with lower dielectric constant and higher packaging density are necessary. The second one is met by decreasing the thermal expansion mismatch between substrate and silicon.

The kaolinite substrate prepared as described in this paper, has the lowest permittivity value obtained to date (Fig. 10) and a thermal expansion very close to that of silicon (Fig. 9). Because of these facts and the low cost of the starting raw materials, this substrate may be of potential interest for the electric and electronic industries.

## Conclusions

Layered kaolinite-alumina ceramics obtained by

sequential slip casting have proved to be a useful model to design new ceramic materials.

A new low-cost ceramic substrate for electronic applications, reinforced by mullite whiskers and with controlled closed porosity, low permittivity value ( $\epsilon \approx 4$  at 1 Mhz) and thermal expansion coefficient close to that of silicon ( $3.8 \times 10^{-6} \text{ }^{\circ}\text{C}^{-1}$ ), has been developed starting from conventional kaolinite powder.

## Acknowledgement

This work was supported by CYCIT Spain under contract MAT-94-0974.

## References

1. Lui, K. C., Thomas, G., Caballero, A., Moya, J. S. & de Aza, S., Mullite formation in kaolinite- $\text{Al}_2\text{O}_3$ . *Acta Metall. Mater.*, **42**(2) (1994) 489-95.
2. Lui, K. C., Thomas, G., Caballero, A., Moya, J. S. & de Aza, S., Time-temperature-transformation curves for kaolinite- $\alpha$ -alumina. *J. Am. Ceram. Soc.*, **77** (1994) 1545-52.
3. Katsuki, H., Furuta, S., Ichinose, H. & Nakao, H., Preparation and some properties of porous ceramics sheet composed of needle-like mullite. *J. Ceram. Soc. Jpn. Int.*, **96** (1988) 1056-61.
4. Leving, E. M., Robbins, C. R. H. & McMurdie, H. F., in *Phase Diagrams for Ceramists*, ed. R. K. Reser, American Ceramics Society, Columbus, OH, 1964, Fig 407.
5. Tummala, R. R., & Rymaszewski, E. J., *Microelectronics Packaging Handbook*, Van Nostrand Reinhold, New York, 1989.
6. Kanzaki, S., Ohashi, M. & Tabata, H., Mullite ceramics for insulating substrates. *Ceram. Trans.*, **6** (1990) 389-99.
7. Giess, E. A., Roldan, J. M., Bailey, Ph. J. & Goo, E., Microstructure and dielectric properties of mullite ceramics. *Ceram. Trans.*, **15** (1990) 167-77.
8. Tummala, R. R., Ceramics in microelectronic packaging. *Am. Ceram. Soc. Bull.* **64**(4) (1988) 752-8.